Conference Proceedings Paper

Classifying UAVSAR PolSAR imagery using target decomposition features

Ghazaleh Alijani [1], Mahdi Hasanlou[2], Zahra Azizi [1]

[1.] Department of GIS/RS, Science and Research Branch, Islamic Azad University, Tehran, Iran, gh.alijani_8016331@yahoo.com, zsazizi@srbiau.ac.ir

[2.] School of Surveying and Geospatial Engineering, College of Engineering, University of Tehran, hasanlou@ut.ac.ir

Abstract: The changes in the earth's surface significantly increase the natural disasters, resulting in severe damage to man-made objects, such as roads, buildings, bridges, and so on. Radar techniques have advantages such as lack of sensitivity to weather conditions, night and day, and cloud cover conditions which can be used to identify, alert, and mitigate these damages. Land use classification due to the importance of these areas and the need to care for them is one of the important applications of remote sensing. Therefore, using polarimetric synthetic aperture radar (PolSAR) images have many capabilities due having the scattering information on the four polarized of HH, HV, VH and VV, and consequently their dependence on the shape and structure of the environment. In this study, UAVSAR image is used. Meanwhile, the support vector machine (SVM) model is one of the well-known classification methods, in addition to being able to run on different types of features from different kinds and in large numbers, which can also distinguish classes those are not linearly separable. On the other hand, it is possible to use data mining method to facilitate data analysis like classification application. In this regards, it is recommended to use random forest (RF) technique. The RF is one of the useful methods for data classification which uses a tree structure for decision making. This method uses strategies to enhance the probability of reaching the goals with conditional probability. In this study, by incorporating a variety of target decomposition methods in PolSAR images, producing the land cover types are generated. Then, using the set of analysis and classification of characteristics, 70 features were obtained by applying SVM, RF, and KNN classification methods. In order to estimate accuracy, the output of these methods was evaluated by reference data.

Keywords: Polarimetric Synthetic Aperture Radar; Classification; support vector machine; random forest; K-nearest neighbors

---

1. MANUSCRIPT

1.1. General Instructions

Today, the use of remote sensing data as an ideal source of precision and speed of operation has become one of the most important means of data collection. In the meantime, radar remote sensing with respect to distinctive features of the capability of capturing images in different weather conditions and throughout the day is becoming widespread. On the other hand, the use of radar polarimetric imaging systems has been widely considered [1] as a result of the use of these images to improve applications such as the use of these images, in order to provide more distributive information about the effects of the image, as well as to distinguish the more similar effects.

Classification is one of the most important techniques for identifying and distinguishing ground type classes that are widely used in the field of geosciences including the use of the classification of images, determining vegetation, determining thermal heat islands, detecting alterations, change detection. Radar images classifying is still interested in the researchers. Yakkekhani et al. (2014) [2] examined the use of the support vector machine (SVM) method with a variety of kernels for classification purposes for the UAVSAR polarimetric data. In 2006, Lardeux et al. [3] proposed an SVM algorithm to categorize all polarimetric data and tested this method on P band data. They showed that the classification of the SVM is better in L band by using the Covariance matrix elements. Khosravi et al. (2014) [4] used a multiple classification systems (MCS) based on the SVM algorithm to classify hyperspectral images. In this research, a comparison was also made between the proposed system and the AdaBoost, Begging and Randomized Forest (RF) methods.

In the previous paragraph, an overview of the research has been briefly described in a variety of classification methods. Although these studies have succeeded in classifying using radar images, they focus on only one classification algorithm. Each of the classification methods has its own special features and applications. Many algorithms are presented for classifying of polarimetric images. One of the most important of these is the K-nearest neighboring (KNN) methods, as well as the SVM and RF algorithm. These three classification methods are recognized as the most suitable models for optimizing the process of classification of remote sensing images [5]. Due to the diversity of methods and the importance of classification using radar data, it is necessary to examine between different classification methods so that users can use the preferred methodology for classification. This research intends to examine types of classification algorithms using UAVSAR radar data. Different types of distribution matrix elements are used for the production of the features. These algorithms used a special manner for producing of the classification map based training data.

The polarization target decomposition divided into four main categories [6]: the first category is based on the dichotomy of Kennaugh matrix that is included Yang, Huynen, Holm, and Brans. The second is developed based on Covariance matrix C3 or coherent matrix that the Freeman Dong decomposition, Durden, and Yamaguchi methods. The third category is worked based on Eigenvector and eigenvalues of covariance matrix or coherence. Some of these methods are applied based on its application such as Holm, Van, Cloud, Zyl and Could, Pottier, and Could. The fourth category of polarization target decomposition is related to the coherent decomposition of S scattering matrix. Some of these methods are Krogager, Cameron, and Touzi [6]. Due to, the presented types of algorithms such as Cloud Pottier, Freeman, Krogager, Van Zyl; presented to produce the features

2. PROPOSED METHOD

2.1. Support vector machine

Support vector machine algorithm is one of the supervised training of pattern detection algorithms which is presented by a Russian mathematician called Vapnik in 1995, and its principles are based on statistical training theory [7]. The main basis of this method is a linear classification of data, by taking safety margins into account, and is basically considered as a binary separator that its main goal of reaching the optimized hyper-plane, as decision level is to increase the boundary of two classes. In case that data are not linearly separated, they are transmitted to higher dimension space using nonlinear kernels, and a hyperplane is formed (Figure 1). Assume that p is a training datum defined as $(x_i.y_i)$, in which x_i is n-dimensional attribution vector, and $y_i \epsilon \{-1.1\}$ is its tag. This hyper-plane is defined by Equation 1:

$$\boldsymbol{w^T}\Phi(\boldsymbol{x}) + \boldsymbol{b} = \boldsymbol{0} \qquad (1)$$

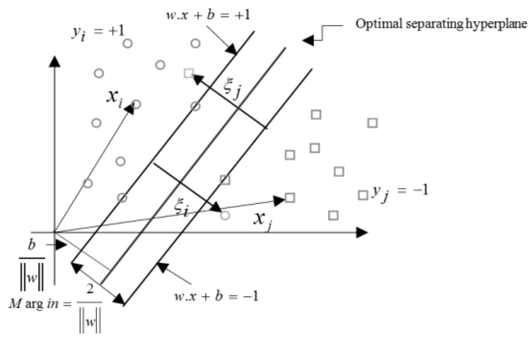

Figure1: Support vector machine classification method.

where w is weight vector which is perpendicular to the intended hyper-plane, b is bias vector which is a constant value showing distance between hyper-plane and origin and $\Phi(x)$ is a kernel to transfer the data to higher dimension space. As been discussed, the aim of this classification is to find a hyper-plane by maximizing the margin and minimizing the overall error of Equation 2.

$$\begin{gathered} \boldsymbol{min}(\frac{\mathbf{1}}{\mathbf{2}}\|\boldsymbol{w}\|^2 + \boldsymbol{C}\sum_{\boldsymbol{i}=\mathbf{1}}^{\boldsymbol{k}}\xi_{\boldsymbol{i}}) \\ \boldsymbol{subjectto}: \boldsymbol{y_i}(\boldsymbol{w}\Phi(\boldsymbol{x_i}) + \boldsymbol{b}) > \mathbf{1} - \boldsymbol{\xi_i}\ \boldsymbol{i} = \mathbf{1} \ldots .\boldsymbol{k} \end{gathered} \quad (2)$$

C is adjusting parameter/factor that adjusts generalization. To consider the noise in the data and interruption between training data, ξ_i is used.

2.2. K-Nearest Neighbour

KNN has been used in statistical estimation and pattern recognition. If training sample of c pairs of random sample $(x_i.y_i)$, in which $i=1,2,\ldots,n$ and label y takes $\{1,2,\ldots,n\}$ values, it can be defined as Equation 3:

$$\begin{gathered} \boldsymbol{train} = \{(\boldsymbol{x_1}.\boldsymbol{y_1}).(\boldsymbol{x_2}.\boldsymbol{y_2}) \ldots .(\boldsymbol{x_c}.\boldsymbol{y_c})\} \\ \boldsymbol{y} = \{\mathbf{1}.\mathbf{2} \ldots .\boldsymbol{n}\} \end{gathered} \quad (3)$$

where y_i determines the class of x_i among the c probable classes. For this reason, for classification, firstly the nearest neighbor x' is determined of X in training samples (Equation 4) [8].

$$\boldsymbol{d}(\boldsymbol{x_i}.\boldsymbol{y_i}) = \sqrt{\sum_{\boldsymbol{r}=\mathbf{1}}^{\boldsymbol{n}}(\boldsymbol{a_r}(\boldsymbol{x_i}) - \boldsymbol{a_r}(\boldsymbol{x_j}))^2} \quad (4)$$

The popularity of this method ensues from two properties, simple application, determined error boundaries. However, high analytical load and high sensitivity to k's value are some of its drawbacks. Therefore, finding k's value has a key role in this method. If k is too small, the algorithm is sensitive to noise and if k is too large, it is possible that among the nearest neighbors, a tag of other classes is entailed.

2.3. Random forest algorithm

Random forest algorithm is one of the recent methods of image classification that is invented by Breiman in 2001 [9], by developing Bagging method. This method differs from Bagging in random feature selection. When creating a decision tree, RF firstly selects a random subset of features in each step of selection branch. The number of trees should be sufficient to fix the error rate [10]. The RF provides more flexible classification, because of selecting randomly subset for producing each decision tree [11].

3. Study area

The data which is used in this research is taken of full polarized data of Panama, the capital city of Panama placed in South America. These data are collected on Feb 6th of February 5, 2010, by UAVSAR Airborne system of JPL institute, NASA. These images are with a spatial resolution of 1.6m in each pixel. The dimension of this datum is 12756×12773 pixels. To reduce the data volume, and consequently reduce the calculation load, a subset with dimension of 276×266 pixels including the urban area, water and vegetation is selected. In Figure 2 and 3, show related Pauli false color image and correspond true color optical image of the considered region on Google Earth. Panama is located on 85°48′20″ W (-85.80556) and 30°10′36″ N (30.17667) geographical longitude and latitude, respectively. The considered region calculation load, a subset with dimension of 276×266 pixels including the urban area, water and vegetation is selected. In Figure 2 and 3, show related Pauli false color image and correspond true color optical image of the considered region on Google Earth. Panama is located on 85°48′20″ W (-85.80556) and 30°10′36″ N (30.17667) geographical longitude and latitude, respectively. The considered region consists of three prominent classes, (1) water, (2) vegetation, and (3) urban area. Ground truth map is produced based on visual comparison and application of high resolution Google Earth images (Figure 5).

Figure 2: Overview of the study area, Pauli false-color image.

Figure 3: True color image of study area (Panama)

4. IMPLEMENTATION

4.1. Extracted decomposition descriptors

To classify the polarimetric image, decomposition descriptor is firstly extracted from the image in the PolSARpro_v4.2.0. To reduce the effect of speckle noise, a filter of 3×3 size on the image for coherent target decomposition descriptors is used.

Table 1: Feature extracted from decomposition

Alpha	**Holm1_T11**	**TSVM_alpha_s2**
anisotropy	**Holm1_T22**	**TSVM_alpha_s3**
beta	**Holm1_T33**	**TSVM_phi_s**
combination_1mH1mA	**Holm2_T11**	**TSVM_phi_s1**
combination_1mHA	**Holm2_T22**	**TSVM_phi_s2**
combination_H1mA	**Holm2_T33**	**TSVM_phi_s3**
combination_HA	**Freeman_Dbl**	**TSVM_psi**
delta	**Freeman_Odd**	**TSVM_psi1**
entropy	**Freeman_Vol**	**TSVM_psi2**
gamma	**Freeman2_Ground**	**TSVM_psi3**
lambda	**Freeman2_Vol**	**TSVM_tau_m**
Huynen_T11	**HAAlpha_T11**	**TSVM_tau_m1**
Huynen_T22	**HAAlpha_T22**	**TSVM_tau_m2**
Huynen_T33	**HAAlpha_T33**	**TSVM_tau_m3**
Barnes1_T11	**Krogager_Kd**	**VanZyl3_Dbl**
Barnes1_T22	**Krogager_Kh**	**VanZyl3_Odd**
Barnes1_T33	**Krogager_Ks**	**VanZyl3_Vol**
Barnes2_T11	**Neumann_delta_mod**	**Yamaguchi3_Dbl**
Barnes2_T22	**Neumann_delta_pha**	**Yamaguchi3_Odd**
Barnes2_T33	**Neumann_psi**	**Yamaguchi3_Vol**

Cloude_T11	**Neumann_tau**	**Yamaguchi4_Dbl**
Cloude_T22	**TSVM_alpha_s**	**Yamaguchi4_Hlx**
Cloude_T33	**TSVM_alpha_s1**	**Yamaguchi4_Odd**
		Yamaguchi4_Vol

4.2. Steps for implementation

When features that are used in decomposition algorithm is extracted, obtained features are overlaid on each other to be applied to the classification algorithm. Using ground optical image matched by radar images, training, and test data are randomly extracted. In this research, 30% and 70% of the values are devoted to training and testing data, respectively. Figure 5 illustrates ground truth map in three classes. Figure 4 presents proposed method flowchart.

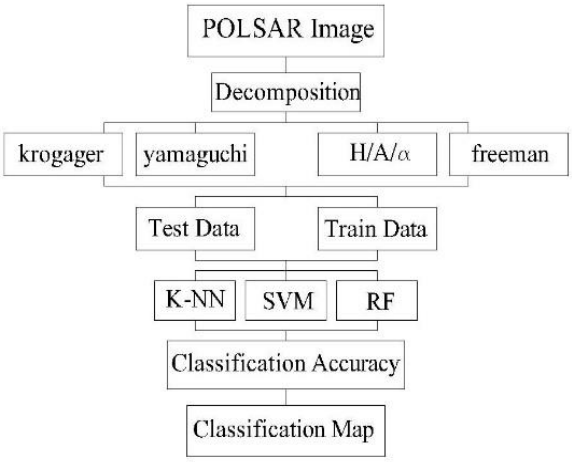

Figure 4: Overview of the proposed method

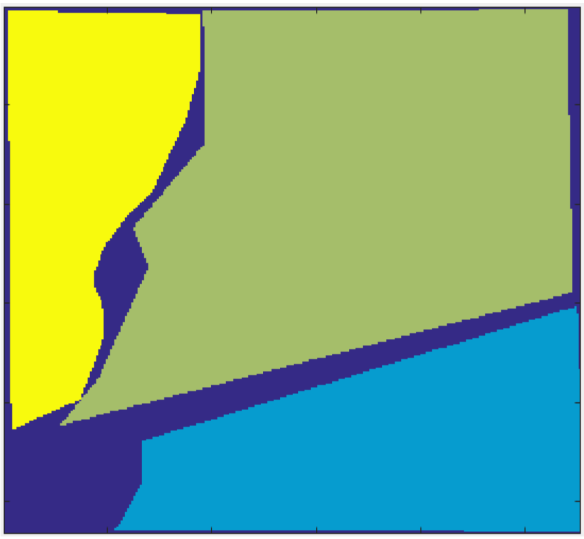

Figure 5: The ground truth dataset.

In this stage extracted features of radar image are introduced as three different classifiers, including SVM, KNN, and RF. Consequently, results of each classifier are examined and evaluated.

One of the supervised image classification methods in this paper is the KNN method. This classification is performed on a SAR image with 70 extracted features. The results of the classification using visual and numerical algorithms were evaluated using an overall accuracy (OA) criteria.

The SVM method has a *C* parameter and its kernel function, which is of the radial basis function kernel (RBF) type, has a parameter γ, which needs to be optimized. For this purpose, a Grid search (GS) was used to determine their optimal values [12]. Also, the RF method has two parameters: the number of trees (N_{tree}) and the number of features in each tree (M_{try}); where necessary, their optimal values are determined. Table 2 presents the optimal values of the parameters of the two methods mentioned.

The quantitative results from the use of classification algorithms are shown in Table 3. Based on numerical results, it is clear that the RF algorithm has a higher degree of accuracy than the other two methods.

Figures 6 through 8 show the visual representation of the algorithms used on the data. Similar to the numerical analysis, the visual results presented performance three of algorithms that show better RF algorithm.

Table 2: The optimal classification parameters.

method	**parameter**	
SVM	C=2	γ=2/4414e-04
RF	N_{tree}=100	M_{try}=8
KNN	K=1	-

Table 3: The classification performance accuracy

Method	**Overall accuracy (%)**
RF	88.65
SVM	77.38
KNN	73.29

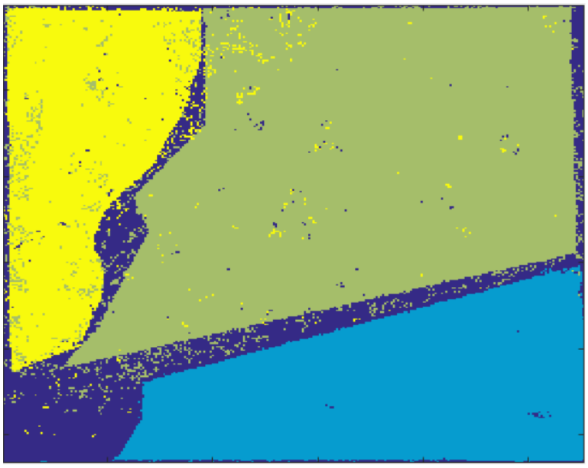

Figure 6: The classified map using the RF method.

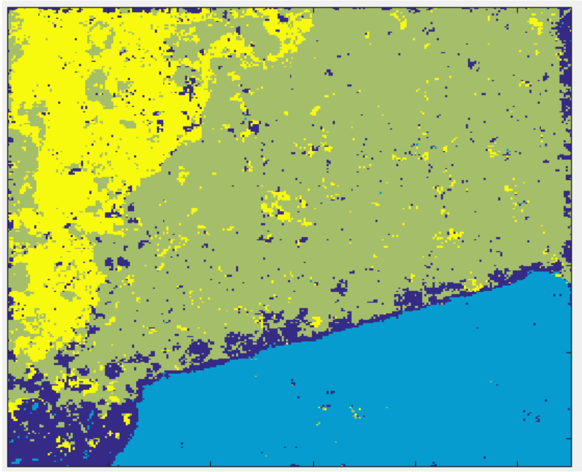

Figure 7: The classified map using the SVM method.

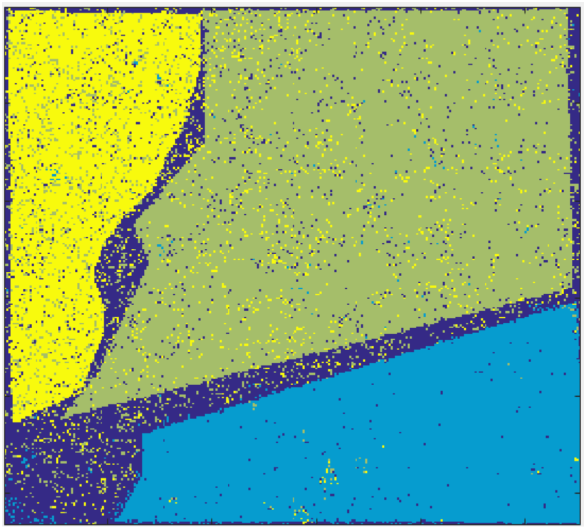

Figure 8: The classified map using the KNN method.

5. CONCLUSION

SAR radar data, and especially all-polar data are used as a relatively new and very useful source of information from the ground due to the features and benefits of the imaging process. In this paper, we examined the classification methods, including SVM, KNN, and RF, in order to compare them with respect to classification speed with appropriate accuracy. For this purpose, the entire polarized image was used in three major classes: urban area, vegetation, and water. After extraction of the characteristic features, each of the mentioned methods for the purpose of classification was applied to the data. The visual and numerical results from the classifications are presented in this study. The RF classification has better classification accuracy than the other two methods. In addition, the RF classification method requires less time to process than other methods. The SVM method in the KNN methodology gives a better accuracy, while it requires high processing time due to the optimization of the parameters.

References

1. Krogager E., Czyz Z.H., 1995, Properties of the Sphere, Diplane Helix Decomposition, Third international workshop on radar polarimetry, (JIPR'95), RESTE, PP. 106-114, Univ. Nantes, France.
2. B. yekkehkhany, S.Homayouni, H. Mcnairn, and A.safari, 'Multi-temporal Full Polarimetry L-Band SAR data classification for Agriculture Land cover mapping, in IGARSS, 2014.
3. C. Lardeux, P.-L. Frison, J.-P. Rudant, J.-C. Souyris, C.Tison, and B. Stoll, "Use of the SVM classification with polarimetric SAR data for land use cartography," in Geoscience and Remote Sensing Symposium, IGARSS 2006.,pp. 493-496, 2006.
4. Khosravi, I., and M. Mohammad-Beigi. 2014. "Multiple Classifier Systems for Hyperspectral Remote Sensing Data Classification." Journal of the Indian Society of Remote Sensing 42(2), 423–428.
5. Thanh Noi, Phan, and Martin Kappas. "comparison of Random Forest, K-Nearest Neighbor, and Support Vector Machine Classifiers for Land Cover Classification Using Sentinel-2 Imagery. "Sensors 2018,18(1), 18.
6. Lee, J.S., Pottier, E., 2009b. .polarimetric radar image : from basics to applications. CRC.
7. V. Vapnik, "The nature of statistical learning theory. 2000," There is no corresponding record for this reference.
8. R. Barandela, and E. Gasca, "Decontamination of training samples for supervised pattern recognition methods." pp. 621-630.
9. Breiman, L., 2003. Manual for setting up, using, and understanding random forest, Remote sensing journal, 4: 23-41.
10. Jin, J., 2012. A Random forest based method for urban land cover classification using LiDAR data and aerial imagery, Remote Sensing of Environment, 81: 190–211.
11. Zhou, Z.H., 2012. In Ensemble methods: foundations and algorithms. Chapman and Hall/CRC Press, 236 pp.
12. M. Hasanlou, F. Samadzadegan, and S. Homayouni, SVM-based hyperspectral image classification using intrinsic dimension, Arabian Journal of Geosciences, vol. 8, no. 1, pp. 477–487, Jan. 2015.

© 2017 by the authors; licensee MDPI, Basel, Switzerland. This article is an open access article distributed under the terms and conditions of the Creative Commons Attribution (CC-BY) license (http://creativecommons.org/licenses/by/4.0/).